**ADVANCED
SCIENCE NEWS**
www.advancedsciencenews.com

**ADVANCED
MATERIALS**
www.advmat.de

COMMUNICATION

Light-Triggered Assembly of Gold Nanoparticles for Photothermal Therapy and Photoacoustic Imaging of Tumors In Vivo

Xiaju Cheng, Rui Sun, Ling Yin, Zhifang Chai, Haibin Shi,* and Mingyuan Gao*

Plasmonic photothermal therapy (PTT) has drawn tremendous attention due to its spatiotemporal addressability, minimal invasiveness, and high therapeutic efficiency for cancer treatment.[1] Gold nanoparticles (AuNPs) have largely been taken as promising photothermal therapeutic agents.[2] However, for spherical solid AuNPs, only those larger than 50 nm present strong near-infrared (NIR) absorption that is essentially required for PTT as well as photoacoustic imaging (PAI). But smaller particles are typically more preferable for tumor theranostic applications owing to their longer blood residence time and shorter biological half-life contrasting to their larger counterparts.[3] In this context, spatiotemporally manipulating the aggregation of small AuNPs in vivo, for shifting the surface plasmon resonance to NIR regions, may offer a solution to solve the above contradiction. Thus far, numerous techniques have been developed for assembling AuNPs into novel functional materials. For example, the assembly of AuNPs can easily be realized in solution by mixing them with multithiol molecules such as dithiol alkane[4] and pentaerythritol tetrakis-3-mercaptopropionate.[5] Unfortunately, this approach is apparently not suitable for forming controllable aggregates of AuNPs in vivo. DNA-mediated assembly of AuNPs at desired locations has been reported for ex vivo diagnostics.[6] But it is technically challenging to apply this approach in vivo due to the costliness, susceptibility to nucleases in blood,[7] and induction of immune response.[8] Stimulus-responsive approaches have recently aroused increasing interests for locally inducing the aggregation of AuNPs at tumorous sites. One of the possible stimuli is the acidic extracellular pH of solid tumors. A number of pH-sensitive AuNPs that can agglomerate at tumorous site have been reported for PTT of cancers.[9] Nevertheless, the sophisticated biological environment may pose unwanted particle aggregation. One way to bypass this hurdle is to utilize light as stimulus because some tumors can spatiotemporally be addressed by light.[10] As a matter of fact, in vitro studies on light-triggered self-assembly of AuNPs have been reported over the past decade based on isomerization or dimerization of light-responsive molecules such as chromophores,[11] spiropyrans,[12] azobenzene,[13] etc. However, in vivo applications of the above-mentioned systems have not been reported before. In addition, the syntheses of the molecular switches involved are often complicated. It is therefore highly meaningful to develop new strategies for spatiotemporally manipulating the assembly of AuNPs in order to achieve aggregates of AuNPs for both PTT and PAI of tumors in vivo.

Herein, we report novel photolabile AuNPs which are covalently cross-linkable with the aid of 405 nm laser irradiation, via a diazirine (DA) terminal group of PEG_{5000} (polyethylene glycol, $M_n = 5000$) ligands on the surface of AuNPs (20.5 nm). As schematically shown in **Scheme 1**, the particle surface diazirine group is first transformed into carbene upon laser excitation at 405 nm. Then, the resulting reactive carbene moieties will form covalent bonds with ligands of adjacent AuNPs through C—C, C—H, O—H, and X—H (X = heteroatom) insertions,[14] leading to the formation of covalently cross-linked particle aggregates, while the AuNPs outside the laser beam will not be triggered. The reason to choose laser instead of conventional light source is that the laser beam can easily be focused to very tiny regions for precise and effective tumor treatment through PTT.

The photolabile AuNPs were prepared as follows. PEGylated AuNPs bearing surface $-NH_2$ groups (denoted as Au@PEG—NH_2 below) were first prepared according to a previously described protocol,[15] and then conjugated with NHS-diazirine (succinimidyl 4,4-azipentanoate) to obtain diazirine-decorated AuNPs (denoted as dAuNPs below). **Figure 1**a shows representative transmission electron microscopy (TEM) images of the resulting dAuNPs together with those obtained after exposure to 405 nm laser irradiation (1 W cm^{-2}) for different periods of time. The average size of the as-prepared dAuNPs is of 20.5 ± 1.9 nm. Upon photoirradiation, the AuNPs did not change much in average size, but largely form particle aggregates and the agglomeration degree of dAuNPs becomes strongly dependent on the exposure time, suggesting that the interparticle cross-linking took place upon laser irradiation.

X. Cheng, R. Sun, Dr. L. Yin, Prof. Z. Chai, Prof. H. Shi, Prof. M. Y. Gao
Center for Molecular Imaging and Nuclear Medicine
School for Radiological
and Interdisciplinary Sciences (RAD-X)
Collaborative Innovation Center of Radiation Medicine
of Jiangsu Higher Education Institutions
Soochow University
Suzhou 215123, China
E-mail: hbshi@suda.edu.cn; gaomy@iccas.ac.cn
Dr. L. Yin
Department of Chemistry and Chemical Engineering
Jining University
Qufu 273155, P. R. China
Prof. M. Y. Gao
Institute of Chemistry
Chinese Academy of Sciences
School of Chemistry and Chemical Engineering
University of Chinese Academy of Sciences
Beijing 100049, China
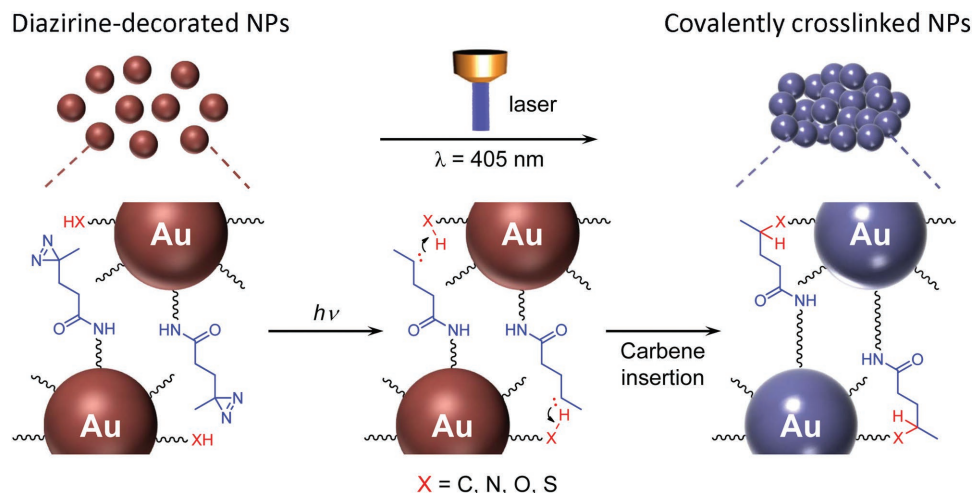
Scheme 1. Schematic illustration of light-triggered assembly of dAuNPs.

To better characterize the aggregating behavior of dAuNPs in solution, dynamic light scattering was carried out to monitor the variation of hydrodynamic size of the resulting aggregates

formed. Figure 1b presents a series of snapshots of the hydrodynamic size profiles recorded at different time points during irradiation. The initial dAuNPs present a symmetric size profile
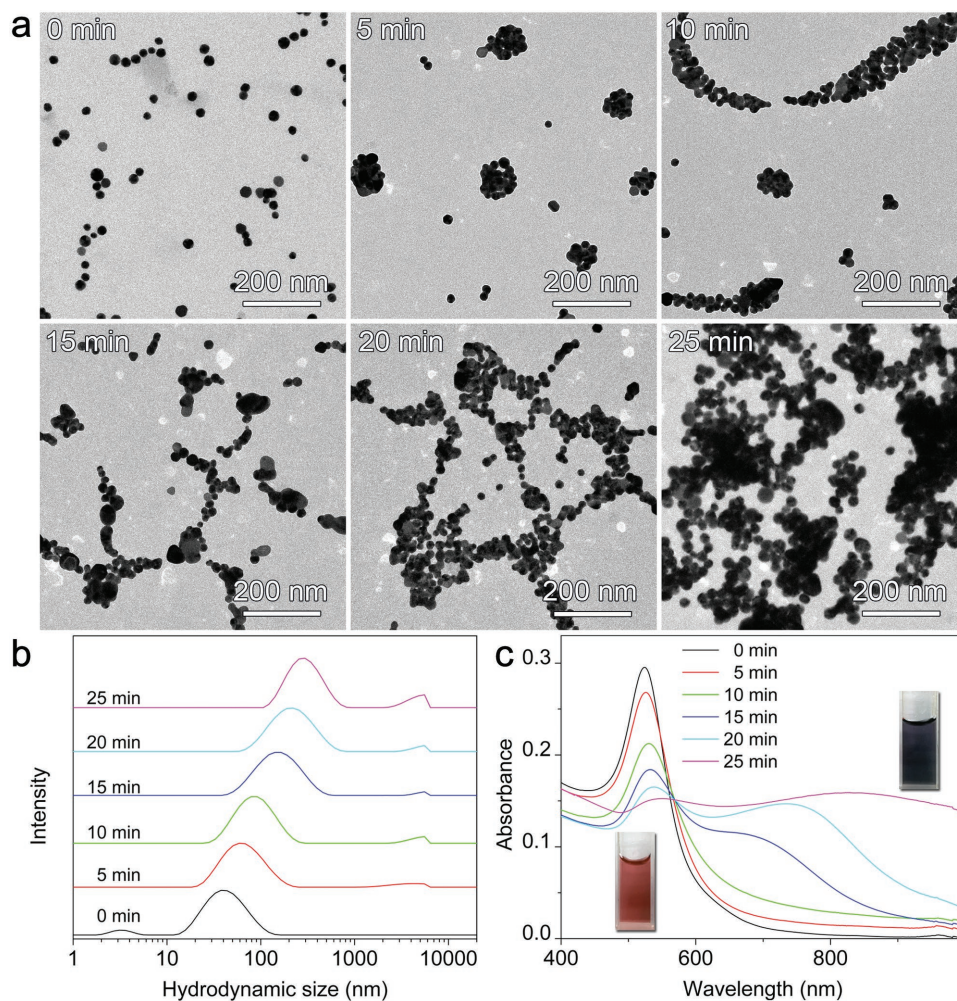

Figure 1. a) TEM images, b) hydrodynamic size profiles, and c) absorption spectra of dAuNPs before and after illuminated with 405 nm laser different periods of time (Inset of panel (c): photographs of aqueous solutions of dAuNPs before and after laser irradiation for 25 min).

**ADVANCED
SCIENCE NEWS**
www.advancedsciencenews.com

**ADVANCED
MATERIALS**
www.advmat.de

COMMUNICATION

with the hydrodynamic size of around 49 nm. Upon irradiation, the hydrodynamic size of dAuNPs quickly increases with irradiation time and eventually reaches 346 nm after 25 min. In contrast, such laser irradiation induced agglomeration was not observed from Au@PEG-NH$_2$ (see Figure S1 in the Supporting Information), which strongly supports that the photoinduced cross-linking of dAuNPs took place via the surface diazirine groups.

Along with the morphological variations, as shown in Figure 1c, the surface plasmon resonance peak, initially locating at around 520 nm for the isolated AuNPs, gradually shifts to longer wavelength. In addition, after ≈15 min of continuous irradiation, a second absorption maximum appears as a shoulder at around 700 nm and gradually extends to NIR region of 700–900 nm against prolonged irradiation. In consequence, the color of the dAuNPs solution was changed from wine red to bluish gray, indicating a strong coupling among particles forming the aggregates. The strong surface plasmon resonance appearing in NIR thus makes the dAuNPs potentially useful for PTT and PAI of tumors. It is deserved to mention that the aggregating behavior induced by laser irradiation could effectively be manipulated through the feeding ratio of DA to PEG−NH$_2$ ligand, denoted as [DA]/[PEG−NH$_2$], as shown in Figure S2 (Supporting Information). Alternatively, the size of the resulting aggregates could also be tuned by the concentration of dAuNPs under fixed feeding ratio of [DA]/[PEG−NH$_2$].

Based on the above optimizations, dAuNPs prepared with [DA]/[PEG−NH$_2$] feeding ratio of 3.6:1 were chosen for the following experiments for evaluating their PTT and PAI performance in vitro. The PA signal of particle aggregates obtained upon laser irradiation for 25 min was recorded against the initial concentration of dAuNPs. As shown in Figure S3 (Supporting Information), the PA signal was remarkably enhanced through the photoinduced aggregation over a large concentration range of dAuNPs. In addition, the PA signal goes linearly with the initial particle concentration, indicating that the light-triggered assembly of dAuNPs can well be controlled. Moreover, the cross-linked AuNPs also presented greatly enhanced photothermal effects contrasting to the noncross-linked ones under 808 nm laser irradiation, as shown in Figure S4 (Supporting Information). For example, after the same dose of 808 nm laser irradiation (1 W cm^{-2}, 5 min), the temperature of the aqueous solution containing cross-linked dAuNPs (150 µg mL^{-1}) was raised to 57.1 °C, while the temperature of the solution containing equal amounts of noncross-linked dAuNPs and pure water was only increased to 30.5 and 26 °C, respectively. Based on a previously reported method,[16] the optical-thermal conversion efficiency (η%) was further estimated to be around 78.8% and 21.6% for the cross-linked dAuNPs and noncross-linked dAuNPs, respectively.

Toward in vivo applications, the cytotoxicity of dAuNPs was first assessed through widely used methy thiazolyl tetrazolium (MTT) assay. As shown in Figure S5 (Supporting Information), dAuNPs exhibited negligible cytotoxicity to 4T1 cells in a concentration range of 12.5–200 µg mL^{-1} after incubated with the cells for 24 and 48 h, respectively. The overall cell viability remained above 80% and prolonged incubation time did not give rise to decreased cell viability. The following TEM studies revealed that dAuNPs after being incubated with 4T1 cells for 24 h could still be cross-linked after being exposed to 405 nm laser light (1 W cm^{-2}, 3 min), while those subjected to no photoirradiation did not show clear aggregation tendency even after being uptaken by 4T1 cells as shown in Figure S6 (Supporting Information).

The photothermal ablation effect of Au particle aggregates on 4T1 cells was then characterized through live/dead staining. The results shown in Figure S7 (Supporting Information) clearly revealed that under safe power density threshold, effective cell thermal ablation could still be achieved with 808 nm irradiation if dAuNPs were precross-linked with 405 nm laser, otherwise no evident cytotoxicity was observed. Further quantified results were obtained through MTT and flow cytometry, as given in Figures S8 and S9 (Supporting Information), respectively, for showing the remarkable photothermal ablation effect of the light-triggered assemblies of dAuNPs in vitro.

The above results firmly demonstrate that the enhanced PAI and PTT capabilities endowed by the light-triggered cross-linking of dAuNPs make the cross-linkable particles promising for tumor theranostics, owing to the expected longer blood circulation time than particle aggregates which are prone to enhanced uptake by reticuloendothelial organs. To show the in vivo application potential, 100 µL of aqueous solution of dAuNPs (2 mg mL^{-1}) was intravenously injected into the tail vein of living female nude mice bearing 4T1 tumors. At 24 h postinjection, the tumorous areas were exposed to 405 nm laser light (1 W cm^{-2}) for 25 min followed by PA imaging. In comparison with control groups, the mice receiving dAuNPs followed by cross-linking process exhibit remarkably increased PA signal at the tumor site, as shown in **Figure 2**a, suggesting that the above laser can effectively induce the cross-linking of dAuNPs in vivo.

In light of these exciting results, the photothermal therapeutic effect of the cross-linked AuNPs was further investigated in vivo. As shown in Figure 2b, the tumor local temperature was raised by 26.7 °C after 10 min of irradiation of 808 nm laser (0.75 W cm^{-2}), while the local temperature of the control tumor was only raised by 8.6 °C upon the same dose of laser irradiation if no precross-linking procedure was applied. To further show the thermal ablation effect in vivo, tumor-bearing BALB/c mice receiving physiological saline (denoted as control), or dAuNPs followed by 405 nm laser irradiation (denoted as dAuNPs+$\lambda_{405\ nm}$), or dAuNPs followed by 808 nm laser irradiation (denoted as dAuNPs+NIR) were set as control groups for showing the treatment efficacy of 808 nm irradiation through AuNPs precross-linked in vivo. The PTT efficacy was evaluated by monitoring the average tumor size of different groups over a period of 20 d. As shown in **Figure 3**a, the tumor size increases in a rather similar way for dAuNPs+$\lambda_{405\ nm}$ and physiological saline groups, while a rather weak inhibition of tumor growth is presented by dAuNPs+NIR group. In huge contrast, the tumors holding cross-linked dAuNPs were effectively reduced in size upon 808 nm irradiation (denoted as dAuNPs+$\lambda_{405\ nm}$+NIR) until three out of four tumors were completely eliminated, as shown in Figure S10 (Supporting Information). The survival rates of mice receiving different treatments are given in Figure 3b. In comparison with control groups, dAuNPs+$\lambda_{405\ nm}$+NIR group exhibits greatly improved survival rate, showing no single death over 20 d.
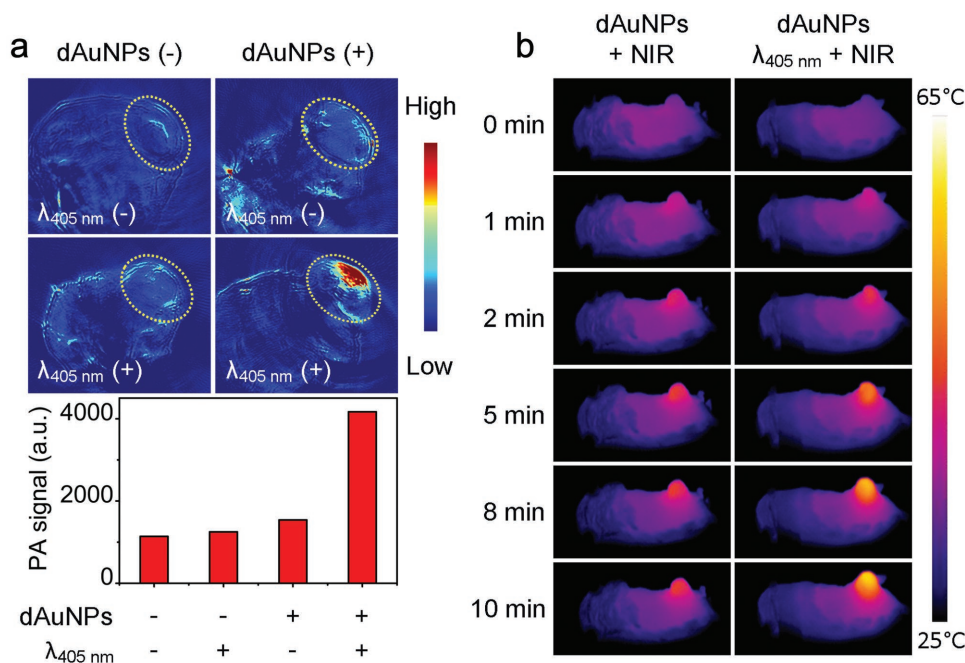
Figure 2. a) PA images and quantified PA signal of the tumorous sites of mice receiving treatments with different combinations of $\lambda_{405\,nm}$ laser irradiation and intravenous delivery of dAuNPs (100 µL, 2 mg mL^{-1}). b) Photothermal images of tumor-bearing mice for showing the in vivo cross-linking effect of dAuNPs on tumor local temperature against irradiation time of 808 nm laser.

To further evaluate the PTT efficacy, tissues of the tumorous sites were extracted on third post-treatment and subjected to hematoxylin and eosin (H&E) staining. As shown in **Figure 4**, no obvious malignant necrosis was observed in the
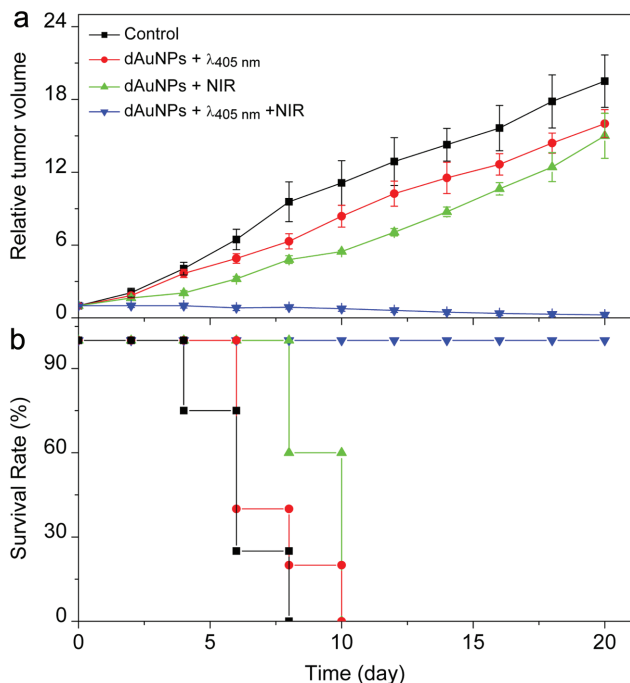

Figure 3. Variation of a) tumor volume and b) survival rate of mice receiving different treatments (n = 4).
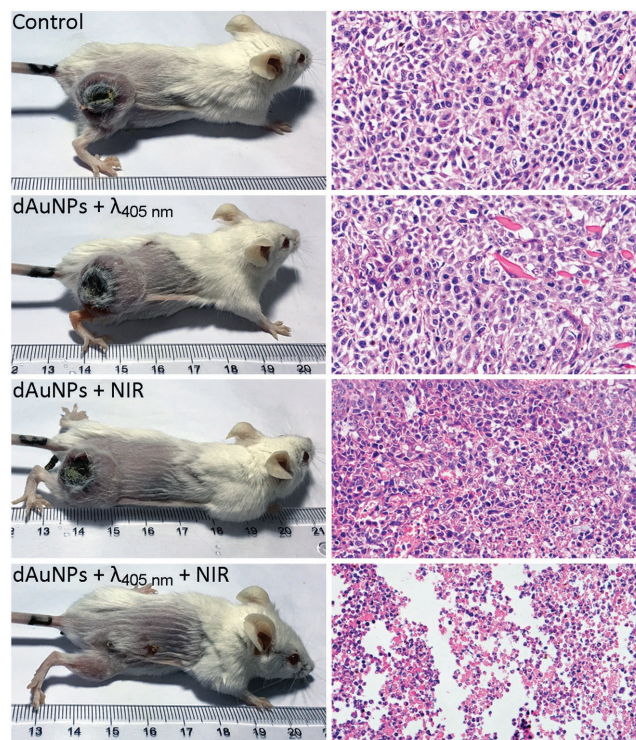

Figure 4. Photographs of representative mice chosen from each group and captured on 20th day post-treatment for showing the therapeutic effects of different therapeutic combinations (left) and slices of tumor tissues extracted on third post-treatment and stained with hematoxylin and eosin (H&E).

control groups of mice, while extensive karyopyknosis and necrosis can be observed from dAuNPs+$\lambda_{405\ nm}$+NIR group, which manifests the excellent PTT efficacy of the cross-linked dAuNPs. All these evidences strongly suggest that the light-triggered assembly of dAuNPs may potentially serve as a platform for effective cancer treatment through PTT apart from enhanced PA imaging. Although the penetration depth of 405 nm laser remains limited (Figure S11, Supporting Information), as a proof of concept study, the current strategy for spatiotemporally manipulating Au particles in vivo can hopefully be extended to other types of photolabile moieties triggerable upon lights with wavelengths more suitable for clinical applications.

In summary, we have successfully developed a novel photo-cross-linkable AuNP. As a gift of the strong coupling among AuNPs cross-linked in vivo, the surface plasmon resonance peak of 20.5 nm AuNPs can effectively be shifted to NIR region, which makes small AuNPs not only useful for enhanced photoacoustic imaging, but also for effective PTT of malignant tumors. We thus believe that the delicate light-addressable cross-linking concept demonstrated herein can potentially be extended into other material systems so as to achieve advanced functions, which are not initially possessed by the building blocks, for biomedical applications.

Experimental Section

Materials: All the chemical reagents were purchased from Sigma-Aldrich and used as received. MTT cell proliferation cytotoxicity assay kit from Sigma, live/dead cell staining kit (calcein-AM-propidium iodide) from Invitrogen, apoptosis detection kit (Annexin V-PE/7-AAD) from BD were used as received.

Preparation of AuNPs: AuNPs were prepared by a classic sodium citrate reduction method according to the previously reported method.[15] In a typical synthesis, 100 mL of Milli-Q water containing ≈0.006 wt% HAuCl$_4$ was heated to boil for 5 min on a hot plate under vigorous stirring. Then, 3 mL of 1 wt% sodium citrate solution was rapidly introduced. The reaction mixture was continuously boiled for another 30 min until the solution changed into wine red and then the reaction was terminated by cooling the reaction system down to room temperature. The resulting AuNP solution was stored at 4 °C for further experiments.

Preparation of NH$_2$-Funtionalized PEGylated AuNPs (Au@PEG—NH$_2$): Into 100 mL aqueous solution of the as-prepared AuNPs, 20 mg of methoxy-PEG$_{5000}$—SH and 20 mg of NH$_2$—PEG$_{5000}$—SH were introduced. The reaction mixture was then kept under stirring overnight to enable the particle surface PEGylation. The resulting PEGylated Au nanoparticles, denoted as Au@PEG—NH$_2$, were purified by repetitive ultrafiltration centrifugation (5000 rpm per 10 min) to remove the unreacted PEG, and then resuspended in Milli-Q water. The percentage of the feeding amount of NH$_2$—PEG$_{5000}$—SH eventually coating on the surface of AuNPs was estimated to be ≈82.2% by analyzing the ultrafiltrate with high performance liquid chromatography (HPLC) after ninhydrin reaction.

Preparation of dAuNPs: Into 1 mL aqueous solution of the as-PEGylated Au@PEG—NH$_2$ (2.48 mg mL^{-1}) containing ≈16.4 mg of NH$_2$—PEG$_{5000}$—SH binding on particle surface, 1.8 µL of NHS-diazirine (1.48 g mL^{-1}) and 3.3 µL triethylamine (0.73 g mL^{-1}) were added. After stirring for 2–3 h at room temperature, the reaction mixture was subjected to ultrafiltration (5000 rpm per 10 min) for three times to afford the desired dAuNPs which were resuspended in Milli-Q water, and stored at 4 °C for further experiments.

Mice Tumor Model: Female BALB/c mice with body weights of 18–20 g purchased from ChangZhou Cavensla Experimental Animal Technology Co. Ltd were housed under standard conditions (25 ± 2 °C/60% ± 10% relative humidity) with 12 h light/dark cycle. The tumors were grafted by subcutaneous inoculation of 1 × 10^6 4T1 cells in about 50 µL phosphate buffered saline (PBS) into the back of each mouse. PAI and PTT studies were carried out when tumor size reached about 50 mm^3. All animal experiment protocols were compliant with the Animal Ethics Committee of the Soochow University Laboratory Animal Center.

In Vivo Photoacoustic Imaging and PTT of Tumors: For in vivo PA imaging, the tumor-bearing nude mice were divided into four groups, and then subjected to different combinations of treatments, i.e., intravenous injection of dAuNPs and 405 nm irradiation. Typically, dAuNPs (100 µL, 2 mg mL^{-1}) were intravenously injected into the tumor-bearing mice. The tumor regions were then exposed to 405 nm laser (1 W cm^{-2}) for 25 min 24 h postinjection. Subsequently, the mice were anesthetized with isoflurane, and placed into a water bath to maintain their body temperature at 37 °C for following tumor imaging.

For in vivo PTT experiments, the tumor-bearing BLAB/c mice were divided into four groups ($n = 4$) and then subjected with different combinations of treatments, i.e., intravenous injection of dAuNPs followed by 405 nm irradiation (denoted as dAuNPs+$\lambda_{405\ nm}$), intravenous injection of dAuNPs followed by 808 nm irradiation (denoted as dAuNPs+NIR), intravenous injection of dAuNPs followed by both 405 and 808 nm irradiation (denoted as dAuNPs+$\lambda_{405\ nm}$+NIR), while mice receiving no treatment served as control. The power density of 808 nm laser for PTT was 0.75 W cm^{-2} and the exposure time was 10 min. The therapeutic effects could be clearly seen from the photographs of typical tumors extracted 20 d post-treatment. Tumor size was measured with a caliper and tumor volume was calculated with the following equation: $V = ab^2/2$, where V is the volume of the tumor, and a and b are tumor length and tumor width, respectively. The tumor volume was continuously monitored till 20 d post-treatment. The tumor tissues were resected from the mice on 3 d post-treatment for evaluating the therapeutic efficacy of different treatments through pathological analysis.

Supporting Information

Supporting Information is available from the Wiley Online Library or from the author.

Acknowledgements

[1] a) M. P. Melancon, M. Zhou, C. Li, *Acc. Chem. Res.* **2011**, *44*, 947; b) V. Shanmugam, S. Selvakumar, C. S. Yeh, *Chem. Soc. Rev.* **2014**, *43*, 6254; c) L. Cheng, C. Wang, L. Feng, K. Yang, Z. Liu, *Chem. Rev.* **2014**, *114*, 10869.

[2] a) R. R. Arvizo, S. Bhattacharyya, R. A. Kudgus, K. Giri, R. Bhattacharya, P. Mukherjee, *Chem. Soc. Rev.* **2012**, *41*, 2943; b) T. L. Doane, C. Burda, *Chem. Soc. Rev.* **2012**, *41*, 2885; c) Y. Xia, W. Li, C. M. Cobley, J. Chen, X. Xia, Q. Zhang, M. Yang, E. C. Cho,

P. K. Brown, *Acc. Chem. Res.* **2011**, *44*, 914; d) R. L. Bardhan, S. Lal, A. Joshi, N. J. Halas, *Acc. Chem. Res.* **2011**, *44*, 936; e) R. A. Sperling, P. R. Gil, F. Zhang, M. Zanella, W. Parak, *Chem. Soc. Rev.* **2008**, *37*, 1896; f) Z. Qin, J. C. Bischof, *Chem. Soc. Rev.* **2012**, *41*, 1191; g) E. Boisselier, D. Astruc, *Chem. Soc. Rev.* **2009**, *38*, 1759; h) L. Dykman, N. Khlebtsov, *Chem. Soc. Rev.* **2012**, *41*, 2256; i) K. Cheng, S. R. Kothapalli, H. G. Liu, A. L. Koh, J. V. Jokerst, H. Jiang, M. Yang, J. B. Li, J. Levi, J. C. Wu, S. S. Gambhir, Z. Cheng, *J. Am. Chem. Soc.* **2014**, *136*, 3560; j) R. R. Xing, K. Liu, T. F. Jiao, N. Zhang, K. Ma, R. Y. Zhang, Q. L. Zou, G. H. Ma, X. H. Yan, *Adv. Mater.* **2016**, *28*, 3669.

[3] C. Y. Liu, Z. Y. Gao, J. F. Zeng, Y. Hou, F. Fang, Y. L. Li, R. R. Qiao, L. Shen, H. Lei, W. S. Yang, M. Y. Gao, *ACS Nano* **2013**, *7*, 7227.

[4] a) I. Hussain, Z. X. Wang, A. I. Cooper, M. Brust, *J. Colloid Interface Sci.* **2006**, *22*, 2938; b) I. Hussain, H. F. Zhang, M. Brust, J. Barauskas, A. I. Cooper, *J. Colloid Interface Sci.* **2010**, *350*, 368; c) P. P. Pillai, B. Kowalczyk, K. Kandere-Grzybowska, M. Borkowska, B. A. Grzybowski, *Angew. Chem. Int. Ed.* **2016**, *55*, 8610; d) H. Deng, F. Dai, G. Ma, X. Zhang, *Adv. Mater.* **2015**, *27*, 3645.

[5] a) R. Klajn, K. J. Bishop, M. Fialkowski, M. Paszewski, C. J. Campbell, T. P. Gray, B. A. Grzybowski, *Science* **2007**, *316*, 261; b) Y. Wang, G. Chen, M. Yang, G. Silber, S. Xing, L. H. Tan, F. Wang, Y. Feng, X. Liu, S. Li, H. Chen, *Nat. Commun.* **2010**, *1*, 87; c) D. Van Haute, J. M. Longmate, J. M. Berlin, *Adv. Mater.* **2015**, *27*, 5158.

[6] a) A. P. Alivisatos, K. P. Johnsson, X. Peng, T. E. Wilson, C. J. Loweth, M. P. Bruchez, P. G. Schultz, *Nature* **1996**, *382*, 609; b) C. A. Mirkin, R. L. Letsinger, R. C. Mucic, J. J. Storhoff, *Nature* **1996**, *382*, 607; c) K. Sato, K. Hosokawa, M. Maeda, *J. Am. Chem. Soc.* **2003**, *125*, 8102.

[7] a) X. Xu, M. S. Han, C. A. Mirkin, *Angew. Chem., Int. Ed.* **2007**, *46*, 3468; b) G. Han, C. T. Martin, V. M. Rotello, *Chem. Biol. Drug Des.* **2006**, *67*, 78.

[8] M. D. Massich, D. A. Giljohann, D. S. Seferos, L. E. Ludlow, C. M. Horvath, C. A. Mirkin, *Mol. Pharm.* **2009**, *6*, 1934.

[9] a) J. Nam, N. Won, H. Jin, H. Chung, S. Kim, *J. Am. Chem. Soc.* **2009**, *131*, 13639; b) X. S. Liu, Y. J. Chen, H. Li, N. Huang, Q. Jin, K. R. Ren, J. Ji, *ACS Nano* **2013**, *7*, 6244; c) S. K. Kang, S. H. Bhang, S. Hwang, J. K. Yoon, J. J. Song, H. K. Jang, S. J. Kim, B. S. Kim, *ACS Nano* **2013**, *9*, 9678.

[10] a) R. Tong, H. H. Chiang, D. S. Kohane, *Proc. Natl. Acad. Sci. USA* **2013**, *110*, 19048; b) X. Z. Ai, J. Mu, B. G. Xing, *Theranostics* **2016**, *6*, 1899.

[11] a) H. B. He, M. Feng, Q. D. Chen, X. Q. Zhang, H. B. Zhan, *Angew. Chem. Int. Ed.* **2016**, *55*, 936; b) Q. Zhang, D. H. Qu, Q. C. Wang, H. Tian, *Angew. Chem., Int. Ed.* **2015**, *54*, 15789; c) T. Bian, L. Shang, H. Yu, M. T. Perez, L. Z. Wu, C. H. Tung, Z. Nie, Z. Tang, T. Zhang, *Adv. Mater.* **2014**, *26*, 5613.

[12] a) P. K. Kundu, D. Samanta, R. Leizrowice, B. Margulis, H. Zhao, M. Börner, T. Udayabhaskararao, D. Manna, R. Klajn, *Nat. Chem.* **2015**, *7*, 646; b) D. Liu, W. Chen, K. Sun, K. Deng, W. Zhang, Z. Wang, X. Jiang, *Angew. Chem., Int. Ed.* **2011**, *50*, 4103; c) Y. Shiraishi, E. Shirakawa, K. Tanaka, H. Sakamoto, S. Ichikawa, T. Hirai, *ACS Appl. Mater. Interfaces* **2014**, *6*, 7554.

[13] a) R. Klajn, P. J. Wesson, K. J. Bishop, B. A. Grzybowski, *Angew. Chem. Int. Ed.* **2009**, *121*, 7169; b) D. Manna, T. Udayabhaskararao, H. Zhao, R. Klajn, *Angew. Chem. Int. Ed.* **2015**, *54*, 12394; c) J. Zhang, Q. Zou, H. Tian, *Adv. Mater.* **2013**, *25*, 378.

[14] a) L. Dubinsky, B. P. Krom, M. M. Meijler, *Bioorg. Med. Chem.* **2012**, *20*, 554; b) H. Shi, C. J. Zhang, G. Y. Chen, S. Q. Yao, *J. Am. Chem. Soc.* **2012**, *134*, 3001.

[15] X. Cheng, X. Tian, A. Wu, J. Li, J. Tian, Y. Chong, Z. Chai, Y. Zhao, C. Chen, C. Ge, *ACS Appl. Mater. Interfaces* **2015**, *7*, 20568.

[16] X. Ding, C. H. Liow, M. Zhang, R. Huang, C. Li, H. Shen, M. Liu, Y. Zou, N. Gao, Z. Zhang, Y. Li, Q. Wang, S. Li, J. Jiang, *J. Am. Chem. Soc.* **2014**, *136*, 15684.